Discovery Nature

To Cite:
Al-Mandalawi M, Sabry Y. Analysis of geotechnical characteristics of open pit rock masses implementing structural discontinuities in the limit equilibrium method. *Discovery Nature* 2025; 2: e15dn3149 doi: https://doi.org/10.54905/disssi.v2i4.e15dn3149

Author Affiliation:
[1]Faculty of Science and Technology, Federation University Australia, Vic, Australia
[2]Al-Faisal College, Auburn, NSW, Australia

***Corresponding Author:**
Maged Al Mandalawi,
Faculty of Science and Technology, Federation University Australia, Vic, Australia,
Email: sp.group@ymail.com

Peer-Review History
Received: 18 June 2025
Reviewed & Revised: 09/July/2025 to 30/November/2025
Accepted: 07 December 2025
Published: 16 December 2025

Peer-Review Model
External peer-review was done through double-blind method.

Discovery Nature
pISSN 2319-5703; eISSN 2319-5711

Analysis of geotechnical characteristics of open pit rock masses implementing structural discontinuities in the limit equilibrium method

Maged Al Mandalawi[1]*, Yasmine Sabry[2]

ABSTRACT

This approach aims to review the structurally controlled instability in the general limit equilibrium method. The fundamental shortage of the finite element technique that simply used static calculations, and does not include discontinuities in the rock mass and treating the rock mass as a continuum. This practical application can overcome the limit of the conventional limit equilibrium method by explicitly including joints and bedding into this method. Rocks are typically anisotropic, and the slope in this study is heterogeneous with joints and faults strike parallel to the orientation in the west wall of Handlebar open pit in Australia. Despite this difficulty, further technique of anisotropic rock mass strength studied to develop the possibility of including joints in the rock slope to evaluate the stability by using the limit equilibrium method LEM. The directional effect of weak structures in a rock mass is typically defined by comparing the results of two sets of strength analyses that govern the two primary failure mechanisms. The first scenario is controlled by two joint sets. The second scenario is controlled by a single dominant bedding plane dips sub–parallel to the slope and one set of joints. The two scenarios represent different geological models, and therefore require rock slope stability analysis methods to determine the critical failure mode. The finding of the analyses shows that the frictional anisotropy influences the location and the scale of the critical slip surface. The dip angle of an apparent structure such as a joint, bedding plane, or fault is often cited as a critical factor controlling the initiation of a rock slope failure surface. This is because the dip angle determines the relationship between the discontinuity and the slope face, directly influencing the shear stress and resistance along the potential failure plane.

Keywords: Slope stability analysis, directional and anisotropic strengths, factor of safety and the limit equilibrium method

1. INTRODUCTION

The presence, orientation, and characteristics of geological discontinuities are the primary controls on most rock slope failures. These structures—such as joints, faults,

bedding planes, and foliation—represent planes of weakness along which failure is most likely to initiate and propagate. The rock failures in local benches or across overall slopes have a high degree of the control of the presence and orientation of discontinuities within the rock mass. Agliardi et al., (2013) summarised three basic considerations for back–analysis of a failure surface. The failure surface can be completely controlled by the structure, partly controlled by the structure, or occur through the low strength rock, or highly fractured rock mass where there is no structural control for the failure mechanism (Pradhan and Siddique, 2020). Read and Stacey (2009) considered that a slope with one discontinuity set parallel to the slope is anisotropic, and the sheer strength of the rock mass would not be isotropic because the slope is weaker in the path of the discontinuity. (Ma et al., 2013) urged that the anisotropic nature of rock where strength properties vary with direction is the primary reason creating challenging to accurately predict its failure process.

The rock mass investigated in Handlebar open pit (Fig. 1) is heterogeneous with highly fractured zones, faults and joints strikes sub–parallel to the orientation of the slope. Therefore, the isotropic strength of the rock mass is integrated into an anisotropic strength model to account for the two rock masses failure mechanisms (Bar and McQuillan, 2018). In this case, the directional effect of the weak structures will be defined by the parameters of the structures or equivalent structures using the following steps:

1. Define the critical structures that dip into the rock mass
2. Define the dip angles of the critical structures, δ_{d1} and δ_{d2}
3. Define the possible variation, $\Delta\delta_d$, of the dip angles of the structures
4. Define the shear strength of the structure, τ_j, and the isotropic strength of the rock mass, τ_{rm},
5. Assign the different domains of the rock mass to other ranges of critical plane orientations to allow simulating composite material that uses varied strength models for variant ranges of orientations.

Figure 1. View of Handlebar open pit, photo taken from the south of the pit.

2. MATERIALS AND METHODS

The limit equilibrium analysis is a common method for assessing the factor of safety FOS using the directional strength of the rock mass as defined by one set of joint, and one set of bedding. The anisotropic strength of the discontinuities and the rock mass which defines the directional strength shows in Fig. 2. The condition of the circle represents the rock mass strength, which differs depending on the

shear strength direction of the structures. The isotropic strength of the rock mass shows as the radius of the circle, while the strength of the structures, d_1 and d_2, displays by the grey and dark–grey rectangles on the side. The definition of the directional strength of a rock mass exhibits joint and bedding sub–parallel to the slope. The radial distance from the centre to the thick curve defines the strength that varies with the inclination of a plane of weakness.

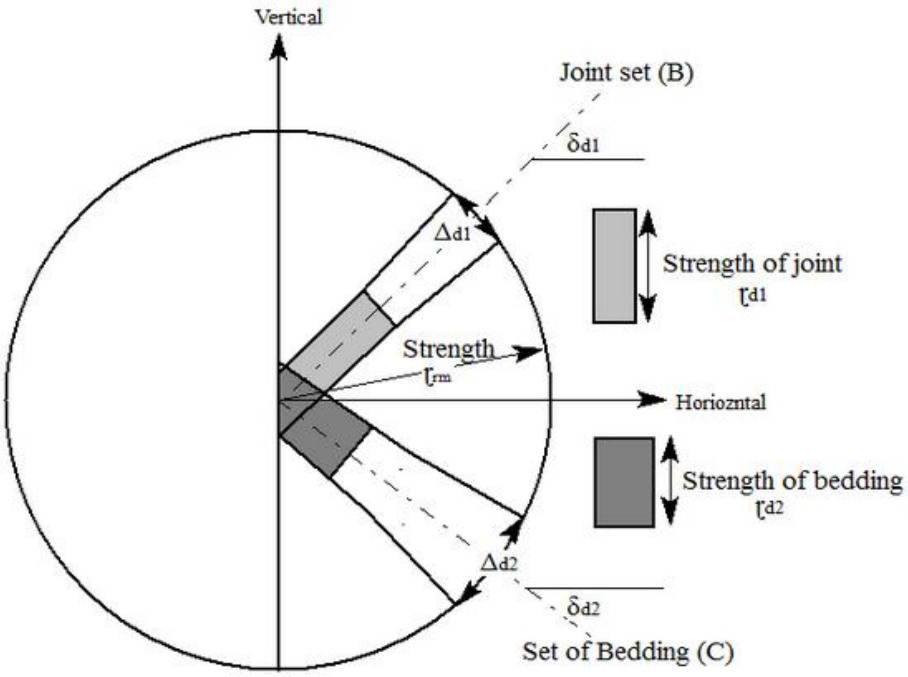

Figure 2. Definition of the directional strength of a rock mass enclosing joint set and set of bedding.

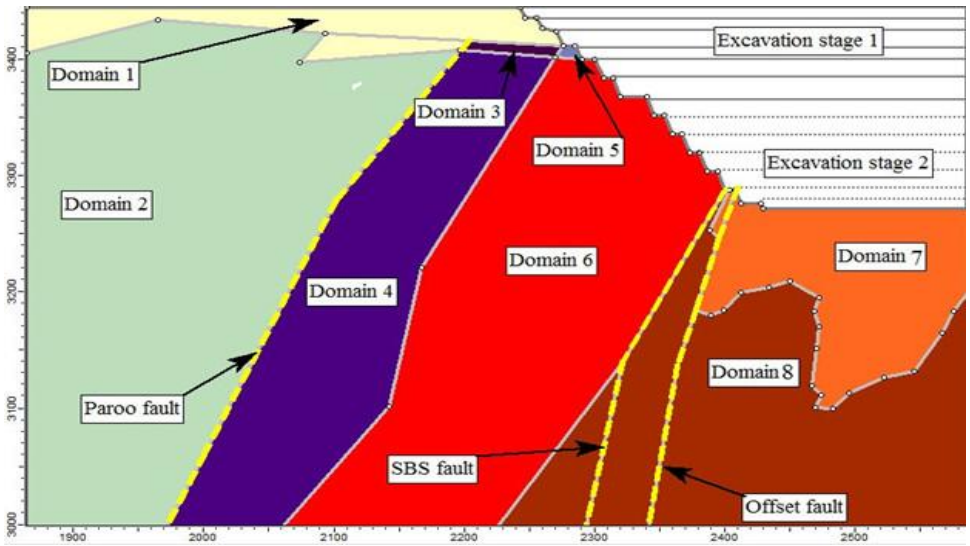

Figure 3. Section through the large–scale faults in the slope.

The limit equilibrium modeling

Rock slope stability analysis is vital role in geotechnical engineering (Ma et al., 2013; Kabeta et al., 2020). The general LEM is still very common because it is a powerful analysis method for non–circular surfaces. A computer program Slide 6.0 has been coded to perform the limit equilibrium calculations with anisotropic material properties definition. This software has a number of options for automatic non–circular critical surface searches, and one of these is the path–search method (Slide 6.0/Rocscience, 2014). A wide range of strength

material models, which designed to specify different material types in different directions, includes the generalised Hoek–Brown failure criterion, and user–defined anisotropic criteria, could be included in this model. When the anisotropic strength function used to simulate the rock mass and planes of weakness of the slope, the GSI was reduced by 20%, compared to the isotropic slopes definition (Marinos et al., 2005). The overall slope angle and the inter–ramp angle of the models are 45° and 49°. The propagation of the tension cracks along the crest with depth of 25m was considered based on the predictions by means of the finite element simulation. Typical details of the slope at the west shows in the pit slope cross-section (Fig. 3). The colours used in Fig. 3 presenting the material properties of the domains that compose the rock masses of the slope. The properties of the materials used in this study are assumed to be fully drained and given in Tables 1 and 3. Table 2 illustrates the colours of the rock domains.

Table 1. Summary of the rock mass properties used in the slope stability analysis.

Domain	Properties	Comments
Fresh Spears Siltstone	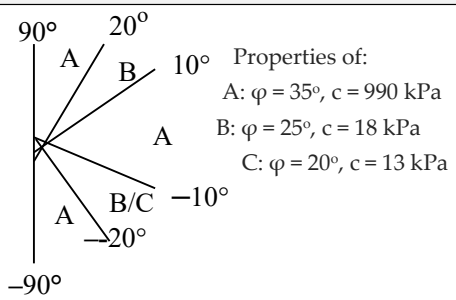 Properties of: A: φ = 35°, c = 990 kPa B: φ = 25°, c = 18 kPa C: φ = 20°, c = 13 kPa	Anisotropic material strength representing the combined properties of the slope rock mass based on the generalized Hoek–Brown criterion, and with two sets of joints (B) or with one set of joints and one set of bedding planes (C).
Leached Urquhart Shale	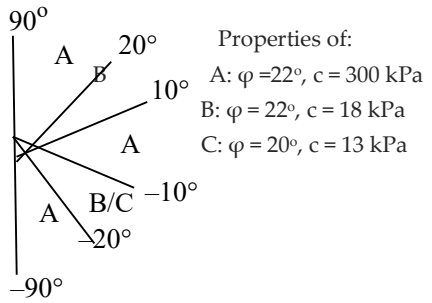 Properties of: A: φ =22°, c = 300 kPa B: φ = 22°, c = 18 kPa C: φ = 20°, c = 13 kPa	Anisotropic material strength representing the combined properties of the slope rock mass based on the generalized Hoek–Brown criterion, and with two sets of joints (B) or with one set of joints and one set of bedding planes (C).
Volcanics Magazine Shale Leached Spears Siltstone Fresh Urquhart Shale	Properties are listed in Table 3	Isotropic strength is representing the properties of intact rock in the slope based on the generalized Hoek–Brown criterion

Table 2. Colours and numbers of materials of the domains of the slope.

Color	Materail name	Domain
	Weathered Volcanics	1
	Fresh Volcanics	2
	Leached Magazine Shale	3
	Fresh Magazine Shale	4
	Leached Spears Siltstone	5
	Fresh Spears Siltstone	6
	Leached Urquhart Shale	7
	Fresh Urquhart Shale	8

Table 3. Parameters of the rock domains for the analysis of the slope.

Parameter	Unit	Domain							
		1	2	3	4	5	6	7	8
γ	KN/m^3	27.4	28.3	26.5	26.5	23.5	27.2	26.9	31.1
φ	(°)	23	32	13	25	20	35	22	44
c	KPa	350	800	50	410	240	990	300	1,250
E_m	MPa	3,000	10,000	4,500	4,500	1,500	8,500	2,000	12,000
Ei	MPa	51,520	76,920	54,050	54,050	31,860	86,640	38,740	102,920
σt	MPa	0.1	0.3	0.0	0.1	0.0	0.4	0.0	0.2
σ_{ci}	MPa	36.4	55.5	32.0	32.0	26.3	111.1	32.7	108
υ	–	0.3	0.2	0.25	0.2	0.25	0.2	0.25	0.2
m_b	–	0.146	0.30284	0.0732	0.2072	0.1148	0.1244	0.1312	0.7617
m_i	–	4	4	4	4	4	4	4	11
s	–	0.000158	0.0011	0.000025	0.0004	0.0001	0.0005	0.00012	0.00086
a	–	0.51168	0.5046	0.5272	0.5076	0.5149	0.5063	0.5131	0.50523
D	–	0.7	0.7	0.7	0.7	0.7	0.7	0.7	0.7
GSI	–	44	59	30	51	40	55	43	58
Dilation	(°)	5	8	4	5	7	12	4	12

3. RESULTS & DISCUSSION

The directional strength model is being used to characterise the material behavior of two different geological units in the pit slope: the fresh Kennedy–Spear Siltstone, and the leached Urquhart Shale. As a result of the weakness of the rock mass in the directions of the joints and bedding, the shear strength for these domains cannot be isotropic. The shear strength of the rock masses are much weaker in the direction of the joint and bedding, and is necessary to be deformed in a butterfly–shaped curve (Read and Stacey, 2009; Chen et al., 2021). While anisotropic models are intended to be more accurate than isotropic ones, results from the anisotropic strength method may underestimate the actual stability behaviour of existing slopes. This is due to how they model the resistance along the failure path, and the assumptions made about the weak planes. The properties of the discontinuities vary considerably across the width of the rock slope. This variation is concluded and studied using two sets of analyses. The first analyses assume that the discontinuity in the plane is controlled by two set of joints (B) in Table 1 with the results given in Fig. 4. The second analysis assumed one set of joints (B), and a set of bedding planes (C) that dip sub–parallel to the slope, and the results illustrated in Fig. 5.

The three critical failure surfaces shown in Fig. 4 indicate that the potential sliding initiated through a combination of sliding along joints, and failure through the rock mass. The calculated deterministic minimum FOS of the slope is 1.137 (in red) for the slope with two joint sets dip into the slope within δ_d = 15°. This slip surface coalesces with a very shallow tension crack at the upper benches and at a point above the ramp. To locate the most critical (least stable) failure path with the lowest FOS, the slip circle/surface grid search method of Rocscience code generated 5,000 random slip surfaces generated, consequently, three typical non–circular surfaces created near the slope surface. The illustration shows a slip surface with FOS of 2.254 passes through the toe in a maximum slope surface depth.

In the model included the bedding planes and joint set dip nearly parallel to the slope shown in Fig. 6, three failure surfaces with a minimum FOS of 1.081. The first model in Fig. 6a shows a plot of FOS = 1.137 for the slope model included bedding planes and joint set dip approximately parallel to the slope δ_d = 15°.

The models shown in Figs. 6b and 6c display the results of the slope with two planes of weakness with orientations of δ_d = 20° and δ_d = 30°, respectively. The three plots shown in

Fig. 6, are representative examples of the influence of increasing the dip angle of the planes on the location, and shape of the peak critical failure surfaces. The localised critical surfaces are initiated in the upper benches of the Spears Siltstone domain of the slope surface, and generated by the directional rock mass strength of this part of the slope.

The directional strength of limit equilibrium results may be changed as a consequence of the spacing of discontinuities in rock mass (Azarafza et al., 2021). The method of excavation, mainly the procedure of explosives, detriments influence on the spacing of rock

discontinuities in the excavation surface. The greatest influence of the method of excavation will be on the spacing of discontinuities. Consequently, applying adjustment factors to the calculated rock mass rating score to account for negative influences into the rock mass classification (Kendorski et al., 1983; Laubscher 1990; Bieniawski, 1989).

Directional cohesion can instantly disturb the inter–ramp, and overall slope equilibrium. Avoiding underestimate the stability of the slope, a new model was considered using a directional cohesion of 68 KPa instead of 18 KPa for the joint sets. An example with an overall slope angle = 45°, φ_d = 25°, c_d = 68 KPa and δ_d = 35° shows in Fig. 7, which can be compared with Fig. 6c where c_d = 18 KPa. The FOS of the slope increases by nearly 14% when the directional shear strength of the discontinuities was increased to 50 KPa. Fredlund (1987) reported that the FOS decreases considerably if the cohesion due to matric pressure reduced during a long-wet period (Li et al., 2021).

The location and profile of the critical localised rock failure surfaces with the lowest FOS stay unchanged. This observation similarly described for soil slopes in geotechnical searches. Zhang (2012) reported that in the soil researches the effect on the location of critical slipping surfaces when using a strength anisotropy function for different values of cohesion is not significant.

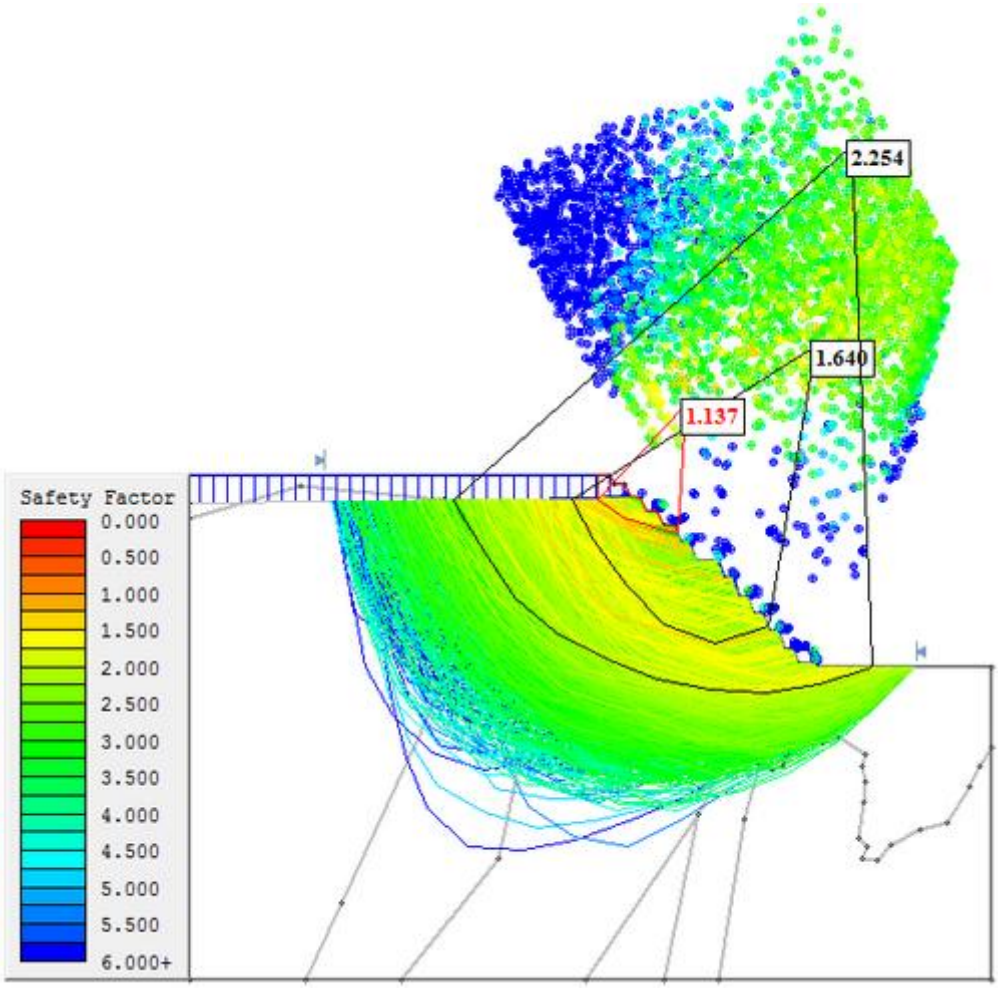

Figure 4. FOS = 1.137 of the most critical failure surface for the slope with the proposed two joint sets dip into the slope within δ_d = 15° and the slope is assumed to be dry. The two critical surfaces illustrated among the 5,000 searched path surfaces; the overall slope angle is 45° and the slope is assumed to be dry.

There is no change in the scale of the most critical failure surface in the slope within the improved anisotropic cohesion strength. This critical sliding surface developed in the weathered Volcanics along the joint sets spacing and coalesces with the intact rock bridges through the fresh Spears Siltstone. The directional cohesion value of the joint initiated this failure surface transition that can dictate the mode of rock failure.

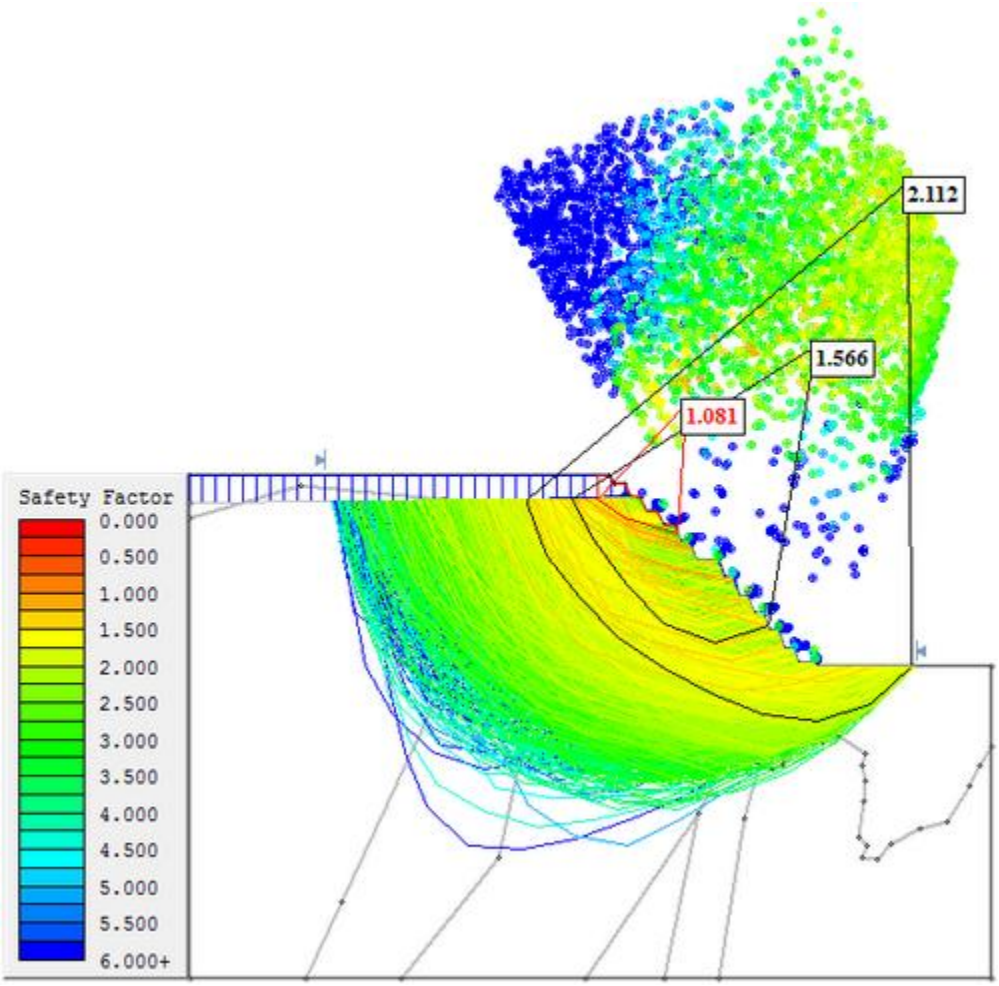

Figure 5. Shows the most critical failure surface for the model with bedding planes and joint set dip approximately parallel to the slope FOS = 1.081. Slip surfaces illustrate the three critical surfaces of the 5,000 searched surfaces. The overall slope angle is 45°, with one joint and bedding both dip into the slope within δ_d =15°, the slope is assumed to be dry.

This stability analysis reached using the LEM proposed by Bishop and showing that the FOS and the slipping surfaces are influenced by the dip angle of apparent structures. The influence of the dip angle of the apparent structures on the FOS becomes more significant than cohesion and other slope parameters. Furthermore, the directional strength method implemented in the limit equilibrium analysis did not describe the coalescence of cracks in the intact rock bridge to generate the shear failure surface of the discontinuity.

Despite the fact that, the joints and bedding sets at the wall of the pit are classified as minor discontinuities and their spacing are slight, there are still several faults, shears, cracks and opening contacts consider as large spacing. Bye and Bell (2001) attributed that different discontinuities and cracks weaken the rock mass and have an essential influence on potential failure mechanisms of rock slopes in open-cut mines. Minor cracks could be associated with fracture spacing and propagate more cracks openings that may potentially initiate critical slipping surfaces (Chan, 2010).

Zhu et al., (2019) investigated the effects of cohesion on the factor of safety of slopes and modeled the critical orientation that typically reduces the FOS. The influence of directional cohesion on the slope's FOS illustrates in Fig. 8. The degradation of directional joint cohesion along the joint surface did not reduce the FOS when the apparent structure dipped at a slight angle. The FOS appears to be intermittently escalated, at first slowly and then more rapidly at a larger directional dip angle. Slope stability was primarily influenced by the dip angle of the apparent structure.

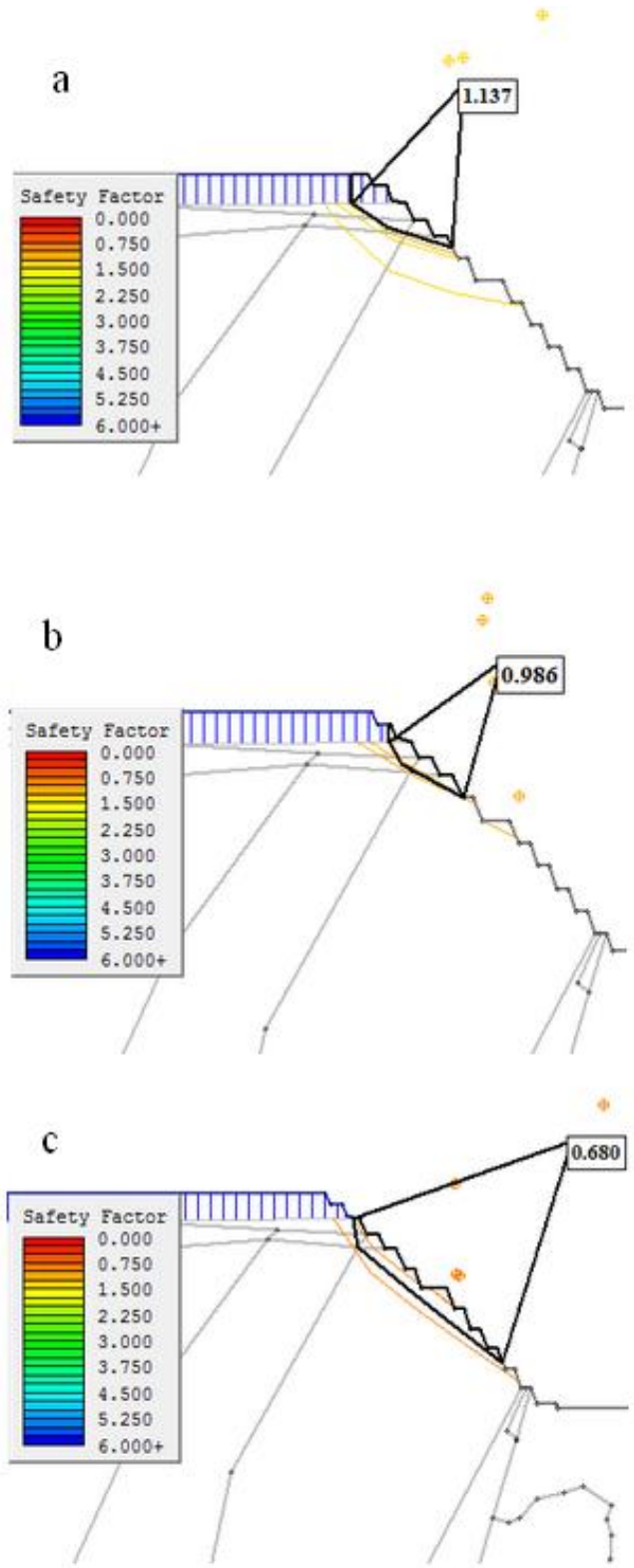

Figure 6. Three most critical surfaces with the lowest FOS for a dry slope with two joint sets dip into the slope within three different dip angles: (a) δd = 15°, (b) δd = 20°, (c) δ_d = 30°.

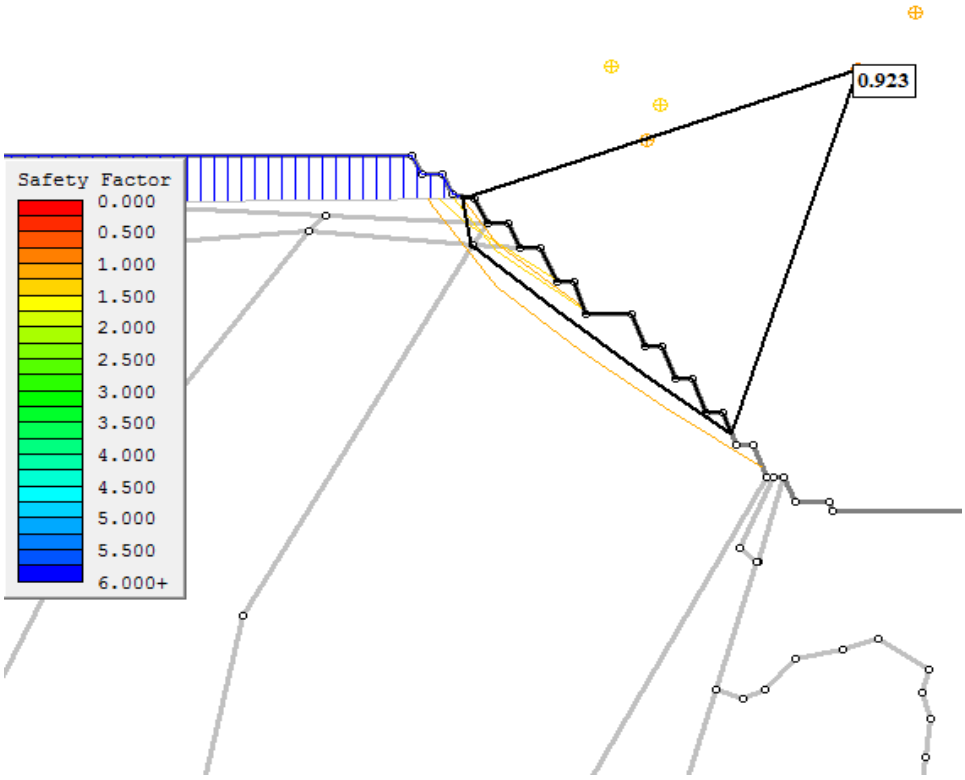

Figure 7. Plot of the five most critical failure surfaces on the slope with increased cohesion force, $\varphi_d = 25°$, $c_d = 68$ KPa, and $\delta_d = 30°$.

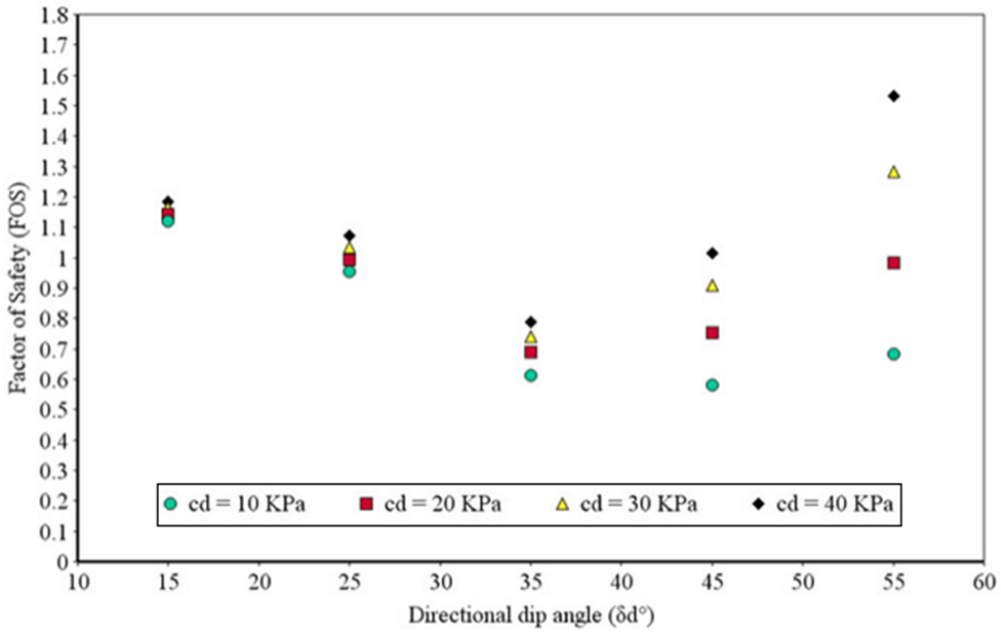

Figure 8. Results of calculations for the slope under dry conditions for different apparent structural dip angles, and predicted FOS using the general LEM, and four different values of directional cohesion.

The shear strength of a rock mass defines by cohesion, and internal friction angle. The previous model focused on the influence of rock strength anisotropy presented as cohesion. In the model in Fig. 9, the effect of rock mass anisotropy and the directional friction angle on the slope stability is calculated, along with the influence on the scale and location of the critical slipping surface.

To take into account the anisotropy in the internal friction angle, the LEM was used, and only the non–circular critical surface search was considered. The shear strength anisotropy in the friction angle is generally correlated with the effective principle stress

condition and the direction of these stresses around a slope (Sjöberg 1997; Karimzadeh et al., 2024). The anisotropy frictional angle value increased to determine the FOS, and the influence of anisotropy of the friction angle on the location of the critical sliding surface. Figure 9 shows the variation of this critical surface when the anisotropy friction angle of the joints φd increased from 25° to 35°, and the cohesion c set to 18 KPa. Misra, and Marangos, (2011) investigated the variation of rock parameters on the slip surface by performing a parametric study using statistical methods.

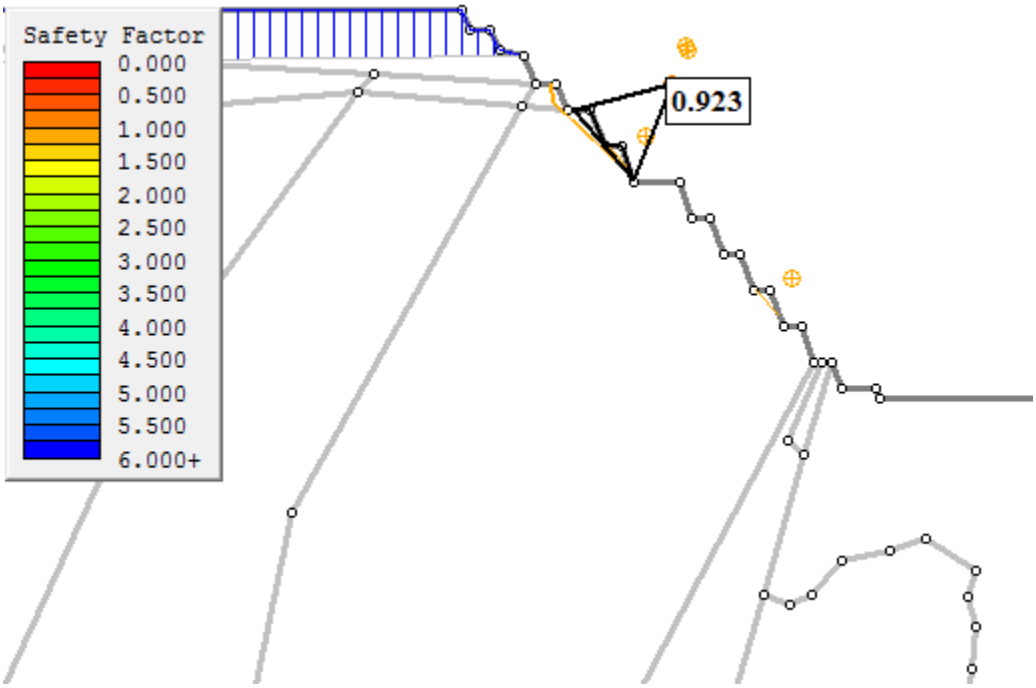

Figure 9. Plot of the five most critical failure surfaces on a bench scale, $\varphi_d = 35°$, $c_d = 18$ kPa, and $\delta_d = 30°$.

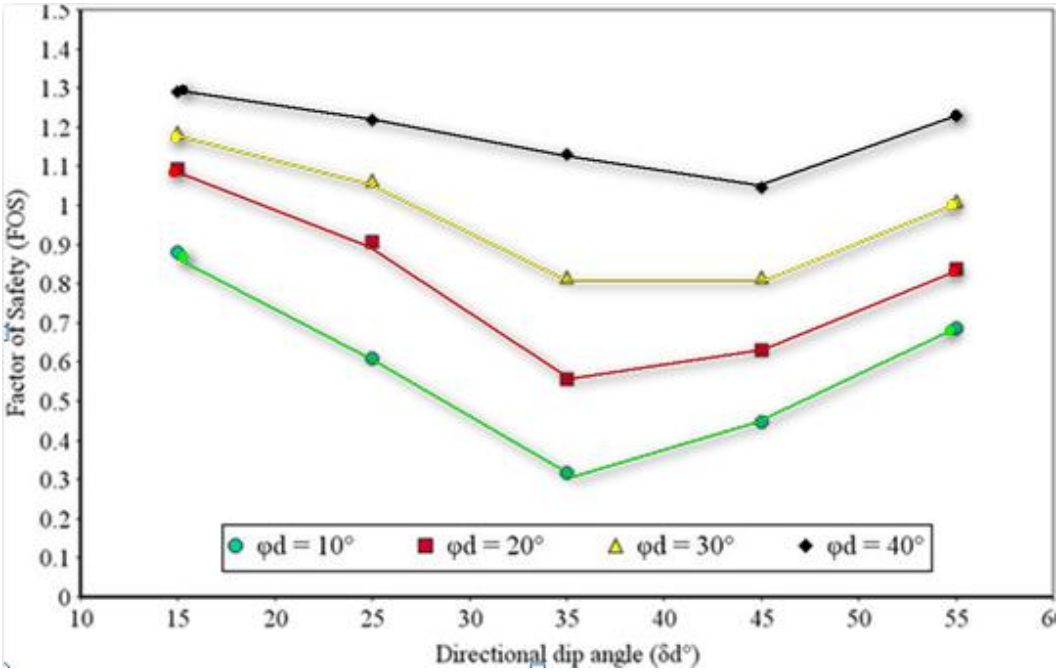

Figure 10. Results of slope calculations for different apparent structural dip angles, and predicted FOS using the general LEM when using four different values of anisotropic internal friction angles.

The overall rock mass response will then correctly represent the effects of joint closure nonlinearity. The scale and location of the critical slipping surface changed dramatically. The line of the most vital surface lengthened between two upper benches on the slope ramp. This is slighter in scale than the critical surface dominated by the increase of directional cohesion. The slope FOS increased to the same value as the model in Fig. 7.

The anisotropy friction angle in the limited equilibrium analysis has an observable influence on the location of the critical sliding surface (Wyllie and Mah, 2004; Rosenkranz et al., 2019). While the slope FOS changed to the limit of the increased directional cohesion slope. The scale of the critical sliding surface reduced from the covering eight benches (in Fig. 7) to covering two upper benches (in Fig. 9). The influence of the anisotropic friction angle on the slope FOS illustrates in Fig. 10.

4. CONCLUSION

The influence of anisotropy of geo-materials on the slope stability due to the dip planes was investigated in the west slope of Handlebar open pit. The anisotropic strength of a rock mass was implemented in limiting equilibrium analysis and performed for the slope with range of directional cohesion, anisotropic friction angles, and different dip angles of apparent structures. Two sets of analyses using LEM code illustrated the models of the findings. The first of these presumed that the discontinuity in the plane of the slope is controlled by two sets of joint, while the second analysis supposed one set of joint and one set of bedding planes that dip approximately sub–parallel to the slope. The obtained local FOS is 1.081 for the worst–case scenario (joint set and bedding) and implicates the local FOS of the failure surfaces generated in the weathered rocks of the Volcanics and the Magazine Shale.

The anisotropy of the internal friction angle in a rock mass causes a significant influence on the stability of slopes. The results show that the frictional of anisotropy rock mass has a major impact on the location, and the scale of the critical slip surface. The influence of the angle of shearing resistance on the stability of jointed rock slopes is generally more dominant than the influence of the cohesion. The apparent dip angle of a weak structure relative to the slope face is often the most crucial factor controlling the initiation of a critical failure surface. Graphical representations of the anisotropic internal friction angle, and directional cohesion demonstrated the inter–relationship between the dip angle of the apparent structure, and the slope's FOS. The approach of using the discontinuities into the limit equilibrium slope stability analysis may be extended into three-dimensional analysis of geotechnical engineering in order to predict of the form and the precise location of rock slope failure probabilities.

Acknowledgement

The authors would like to express their appreciation to Glencore zinc for providing permission to carry out this research and publish this paper.

Informed consent

Not applicable.

Ethical approval

Not applicable. This article does not contain any studies with human participants or animals performed by any of the authors.

Conflicts of interests

The authors declare that they have no conflicts of interests, competing financial interests or personal relationships that could have influenced the work reported in this paper.

Funding

This research did not receive any external funding like specific grant from funding agencies in the public, commercial, or nonprofit sectors.

Data and materials availability

All data associated with this study will be available based on the reasonable request to corresponding author.

REFERENCES AND NOTES

1. Agliardi F, Crosta GB, Meloni F, Valle C, Rivolta C. Structurally-controlled instability, damage and slope failure in a porphyry rock mass. Tectonophysics. 2013;605:34-47.
2. Azarafza M, Akgün H, Ghazifard A, Asghari-Kaljahi E, Rahnamarad J, Derakhshani R. Discontinuous rock slope stability analysis by limit equilibrium approaches–a review. International Journal of Digital Earth. 2021;14(12):1918-41.
3. Bar N, McQuillan A. 3D limit equilibrium slope stability analysis for anisotropic and faulted rock masses in Australian coal and iron ore mines. InISRM International Symposium-Asian Rock Mechanics Symposium 2018 Oct 29 (pp. ISRM-ARMS10). ISRM.
4. Bieniawski ZT. Engineering rock mass classifications: a complete manual for engineers and geologists in mining, civil, and petroleum engineering. John Wiley & Sons; 1989 Aug 24.
5. Bye AR, Bell FG. Stability assessment and slope design at Sandsloot open pit, South Africa. International Journal of Rock Mechanics and Mining Sciences. 2001;38(3):449-66.
6. Chan KS. Roles of microstructure in fatigue crack initiation. International Journal of Fatigue. 2010;32(9):1428-47.
7. Chen S, Xia Z, Feng F, Yin D. Numerical study on strength and failure characteristics of rock samples with different hole defects. Bulletin of Engineering Geology and the Environment. 2021;80(2):1523-40.
8. Fredlund DG. Slope stability analysis incorporating the effect of soil suction. Slope stability. 1987:113-44.
9. Kabeta WF, Diro GA, Teshager DK. Assessments of geotechnical conditions and slope stability analysis: case study in gedo town, Ethiopia. Int. J. Sci. Res. Eng. Trends. 2020;6(3):1250-8.
10. Karimzadeh AA, Leung AK, Gao Z. Shear strength anisotropy of rooted soils. Géotechnique. 2024;74(10):1033-46.
11. Kendorski FS, Cummings RA, Bieniawski ZT, Skinner EH. Rock mass classification for block caving mine drift support. InISRM Congress 1983 Apr 10 (pp. ISRM-5CONGRESS). ISRM.
12. Laubscher DH. A geomechanics classification system for the rating of rock mass in mine design. Journal of the Southern African Institute of Mining and Metallurgy. 1990;90(10):257-73.
13. Li Y, Satyanaga A, Rahardjo H. Characteristics of unsaturated soil slope covered with capillary barrier system and deep-rooted grass under different rainfall patterns. International Soil and Water Conservation Research. 2021;9(3):405-18.
14. Ma K, Tang CA, Li LC, Ranjith PG, Cai M, Xu NW. 3D modeling of stratified and irregularly jointed rock slope and its progressive failure. Arabian Journal of Geosciences. 2013;6(6):2147-63.
15. Marinos VI, Marinos P, Hoek E. The geological strength index: applications and limitations. Bulletin of Engineering Geology and the Environment. 2005;64(1):55-65.
16. Misra A, Marangos O. Rock-joint micromechanics: relationship of roughness to closure and wave propagation. International Journal of Geomechanics. 2011;11(6):431-9.
17. Pradhan SP, Siddique T. Stability assessment of landslide-prone road cut rock slopes in Himalayan terrain: a finite element method based approach. Journal of Rock Mechanics and Geotechnical Engineering. 2020 Feb 1;12(1):59-73.
18. Read J, Stacey P. Guidelines for open pit slope design. CSIRO Publishing/CRC Press, 2009.
19. Rosenkranz A, Costa HL, Profito F, Gachot C, Medina S, Dini D. Influence of surface texturing on hydrodynamic friction in plane converging bearings-An experimental and numerical approach. Tribology International. 2019;134:190-204.
20. Sjöberg J. Estimating rock mass strength using the Hoek–Brown failure criterion and rock mass classification—a review and application to the Aznalcollar open pit. Division of Rock Mechanics, Department of Civil and Mining Engineering, Lulea University of Technology, Sweden. 1997.
21. Slide 6.0/Rocsience. 2D The Limit Equilibrium Slope Stability Analysis. User's manual. Rocscience INC, Toronto, Canada, 2014.
22. Wyllie DC, Mah CW. Rock slope engineering: civil and mining—4th ed. p. cm. India, Newgen Imaging Systems (p) Ltd, Chennai. 2004.
23. Zhang LW. Influence of anisotropic internal friction angle on the stability of uniform soil slopes. Applied Mechanics and Materials. 2012;170:270-3.
24. Zhu H, Zhang LM, Xiao T. Evaluating stability of anisotropically deposited soil slopes. Canadian Geotechnical Journal. 2019;56(5):753-60.